Appl. Phys. B 53, 23–29 (1991)

Applied Physics B Photophysics and Laser Chemistry

Temperature Measurement by Single-Shot Dual-Line CARS in Low-Pressure Flows

M. Péalat and M. Lefebvre

Office National d'Etudes et de Recherches Aérospatiales, BP 72, F-92322 Châtillon Cedex, France

Received 2 January 1991/Accepted 12 April 1991

Abstract. A CARS method, adapted for diagnostics in low-pressure unsteady flows is described. The technique employs two narrow-band dye lasers and a single-frequency pump laser. Single-shot rotational temperature is obtained from the ratio of the intensities of two isolated Q lines. Temperature-measurement accuracy is discussed. The advantage of referencing the CARS signals from the flow in a cell filled with the same gas is shown. Demonstrative experiments are performed using N_2 at pressures of 10^2–10^3 Pa.

PACS: 07.60, 82.80

Renewed interest in suborbital aircrafts and space shuttles stimulates development of diagnostics for wind tunnels and shock tubes. Among the optical diagnostics techniques capable of non-intrusive measurements, Raman scattering and laser-induced fluorescence techniques have received attention recently [1–3]. Coherent Anti-Stokes Raman Scattering (CARS) is one of the Raman processes which allow spatially-resolved and time-resolved concentration and temperature measurements. Since the first demonstration of the potential of CARS in 1973 [4], many studies have been carried out with CARS setups equipped with pulsed lasers, mainly in combustion research and plasma physics. Two methods have been used to record the CARS spectra [5]. The first one, called scanning CARS, uses a monochromatic laser and a tunable narrow-band laser; it has a detection limit of the order of 10^{14} cm^{-3} but, because the spectral analysis takes several minutes, only stable or reproducible media can be studied. The second method, called broad-band CARS, is well suited to study fluctuating or transient phenomena. It requires a monochromatic laser and a laser covering a wide range of frequencies. The entirety of the CARS spectrum is generated during a single laser shot. The laser energy being now spread over a wide spectral domain, the CARS signal spectral intensity is reduced by several orders of magnitude. The detection limit increases to 10^{17} cm^{-3}.

Neither broad-band nor scanning CARS can be used to perform measurements in low-pressure unsteady reacting system such as hypersonic flows. Firstly, the number densities are too low for broad-band CARS; secondly the run durations are generally too brief for scanning CARS. We propose in this paper a new CARS technique, called dual-line CARS, in which two Q line intensities are measured simultaneously. It has the detectivity limit of scanning CARS and is capable of brief, i.e. 10 ns, temperature measurements. The approach of using a two-color dye laser instead of a broad-band dye laser was proposed by Aldén et al. [6] for fast temperature determination by CARS in combustion experiments. However, the standard deviation of temperature measurements was 50% greater than that obtained by using a broad-band dye laser and making a complete regression analysis [7]. A similar method although not yet experimentally demonstrated to our knowledge has also been proposed for instantaneous temperature measurement by laser-induced fluorescence [8].

The first part of this communication is devoted to the principle of the dual-line CARS technique. Then the main sources of CARS signal fluctuations which has precluded up to now dual-line CARS to be used for accurate temperature measurements are developed. Referencing the CARS signals in a cell containing a sample of the gas under study is shown to reduce noise and systematic errors. Finally an experiment demonstrating the feasibility of dual-line CARS is presented.

Principle

The idea which supports the dual-line CARS technique is simple: the rotational temperature is deduced from the

ratio of the intensities of the $Q(J)$ and $Q(J')$ rotational lines simultaneously measured. The dual line CARS technique requires three pulsed lasers of frequencies ω_1, ω_2, and ω_2'. Two CARS signals are generated if ω_2 and ω_2' are tuned so that $(\omega_1-\omega_2)$ and $(\omega_1-\omega_2')$ are resonant with the Raman frequencies ω_J and $\omega_{J'}$ of the rotational lines $Q(J)$ and $Q(J')$ in the fundamental vibrational band $v=1\leftarrow v=0$. v and J are the vibrational and rotational quantum numbers of the lower state of the $Q(J)$ transition, and (v, J') are those of the $Q(J')$ line.

Low densities constitute the domain of interest for dual-line CARS; then Q rotational lines are isolated and the CARS signals are proportional to the square of the density, and depend on the rotational state population distribution. Then it is obvious that the rotational temperature may be obtained from the ratio of two isolated rotational intensities even if the density of the medium is unknown. However, since each CARS signal is noisy, the ratio fluctuates and consequently also the temperature deduced from this ratio. Until now, the CARS signal noise has precluded use of dual-line CARS [7].

Assuming the $Q(J)$ rotational line to be isolated and the ω_1 laser to be single mode, the $Q(J)$ CARS signal is obtained from (similar development applies for J'):

$$S(\omega_1-\omega_2)=K_S(\Delta N_J^S\sigma_J)^2 S_{AT}(\omega_1-\omega_2)\int_{\Delta t} dt\, P_1^2 \times\sum_k P_2^k\left|\int\frac{g(v_z)dv_z}{(\omega_1-\omega_2^k)-\omega_J\left(1-\frac{v_z}{c}\right)-i\Gamma_c}\right|^2 \quad (1)$$

where the summation integrates the contribution of each mode ω_2^k of the ω_2 laser (central frequency: ω_2) and the integral describes the Raman line profile [9]. The Doppler shift is represented by $\omega_J v_z/c$ where v_z is the projection of the velocity vector on to the wave-vector difference $\vec{K}_1-\vec{K}_2$, and $g(v_z)$ is the Maxwell-Boltzmann distribution function. Γ_c is the collisional broadening (half width at half maximum HWHM). We also use below the Doppler broadening (HWHM) $\Delta\omega_D$.

- $S_{AT}(\omega_1-\omega_2)$ represents the effect of saturation, i.e. the Raman population pumping and the Stark shift [10]. This factor is introduced because (1) is derived from a perturbation-theory calculation which supposes weak laser fields. In contrast, in real experiments, the gas pressures are low and strong laser fields are needed to create a measurable signal, which leads to saturation. More precisely, S_{AT} phenomenologically describes the deviation of the CARS signal strength from the classical $P_1^2P_2$ dependence. Without saturation effects, $S_{AT}=1$. With saturation, the value of S_{AT} depends on many experimental parameters: the laser pulse duration, the diameter of the laser foci, the relationship between the phases of the ω_2^k modes and the detunings from resonance $[(\omega_1-\omega_2^k)-\omega_J]$. To treat saturation in an exact manner, one should solve the time evolution of the density matrix equations for each velocity group [11].
- K_s is a proportionality factor which takes into account the optical transmission of the signal channel, the quantum efficiency of the detector at the central anti-Stokes frequency $\omega_3=2\omega_1-\omega_2$ and the probe volume geometry.
- σ_J is the spontaneous Raman scattering cross-section; ΔN_J^S is the population difference between the $(v=0, J)$ and $(v=1, J)$ states.
- P_2^k is the power of the k^{th} mode at the frequency ω_2^k of the ω_2 laser. P_2^k has a Gaussian temporal behavior:

$$P_2^k=\hbar\omega_2^k n_2^k\pi^{-1/2}\tau_p^{-1}\exp[-(t/\tau_p)^2] \quad (2)$$

where n_2^k is the total number of photons in the k^{th} mode, $\hbar$ the Planck constant and τ_p the pulse duration. The net ω_2 power is $P_2=\sum_k P_2^k$.

- P_1 is the ω_1 laser power. Its time dependence obeys an equation similar to (2), where n_2^k is replaced by n_1, number of ω_1 photons.
- We also define the power densities I_1, I_2, and I_2^k using $I_1=P_1/\pi r^2$, $I_2=P_2/\pi r^2$, and $I_2^k=P_2^k/\pi r^2$ where r is the radius of the probe volume at half maximum.

Main Sources of CARS Signal Fluctuations and Practical Solution

It is well known that the CARS signals $S(\omega_1-\omega_2)$ and $S(\omega_1-\omega_2')$ suffer large shot-to-shot fluctuations, larger than those due to Poisson statistics. CARS signals usually vary between 1 and 3 for successive laser shots which makes it difficult to use of dual line CARS without precautions. The expression (1) allows us to understand more precisely the origins of these shot-to-shot fluctuations.

1) K_s undergoes changes because the directions and the aberrations of the laser beams vary slightly; this modifies the phase and intensity distribution within the probe volume and its boundaries. These changes have several causes, such as fluctuations in the pump energy or cooling of the Nd:YAG laser rods, or turbulence in the dye flows.

2) P_1 and P_2^k vary according to their statistical behaviors. The statistical behaviors of the shot-to-shot values of n_1 and n_2^k are different. Because the ω_1 laser is single mode, the fluctuations in the number of photons n_1 are small whereas the shot-to-shot fluctuations of n_2^k are very large although Σn_2^k varies very little. More precisely, the probability for the k^{th} mode to have n_2^k photons is given by the Laplace law [12]:

$$\text{Prob}(n_2^k)=\langle n_2^k\rangle^{-1}\exp[-(n_2^k/\langle n_2^k\rangle)] \quad (3)$$

where $\langle n_2^k\rangle$ is the average number of photons in the k^{th} mode.

The envelope of the spectral distribution of the $\langle n_2^k\rangle$ amplitudes is supposed to be Gaussian:

$$\langle n_2^k\rangle=\exp[-(\Delta\omega_2^k/\Gamma\omega_2)^2] \quad (4)$$

where $\Delta\omega_2^k=\omega_2^k-\omega_2$ and $\Gamma\omega_2$ is the half width at 1/e of the laser line.

Indeed, the changes of P_2^k constitute the main source of fluctuations when the Raman linewidth is smaller than the free spectral range between the ω_2^k modes or comparable to it (Fig. 1). This is the situation encountered in a low-

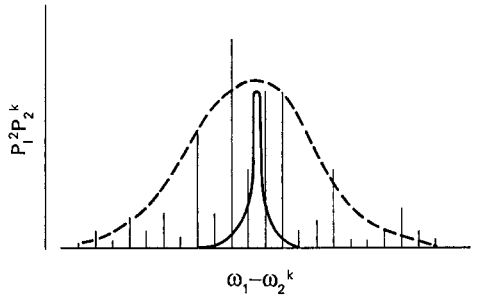

Fig. 1. Schematic of the laser product $P_1^2P_2^k$ versus the frequency difference $(\omega_1-\omega_2^k)$. The dashed line is the Gaussian envelope which would be obtained by averaging many laser shots. The full line is the Raman lineshape, i.e. the squared modulus in (1)

pressure N_2 flow where for 10^3 Pa of pure N_2 at 300 K, $\Gamma_c \ll \Delta\omega_D$ with $\Delta\omega_D = 5\cdot 10^{-3}$ cm^{-1} whereas the free spectral range between the laser modes is $\sim 10^{-2}$ cm^{-1}. Then, few ω_2 modes contribute to the CARS signal and consequently, the statistical distribution of the CARS signal amplitude is comparable with those of n_2^k. It may be pointed out that the situation differs for laser induced fluorescence, because the UV transitions are broader; thus, a large number of independent laser mode contributions are averaged, which reduces the statistical signal fluctuations.

3) S_{AT} fluctuates because P_1 and P_2 have global variations from shot to shot, but also primarily because the Stokes k modes undergo fluctuations in their frequencies ω_2^k, phases φ_2^k and amplitudes n_2^k; thus, for the same P_1 and P_2, there are signal variations because the lines are excited in or out of resonance and because the most resonant mode is more or less powerful.

A solution, now currently used, partially solves the problem. It consists in dividing the sample signal $S(\omega_1-\omega_2)$ by a reference CARS signal $R(\omega_1-\omega_2)$ measured simultaneously with $S(\omega_1-\omega_2)$. The reference signal is created in a cell filled with a rare gas. It is given by

$$R(\omega_1-\omega_2)\alpha\int dt P_1^2 P_2 . \tag{5}$$

We see that $S(\omega_1-\omega_2)/R(\omega_1-\omega_2)$, which contains the required spectral information, is partially independent of P_1 and P_2^k. Moreover, beam aberrations and beam overlap are partially compensated for, because $R(\omega_1-\omega_2)$ is also created by a CARS process. Standard deviations of the order of 30% are generally observed for the ratio $S(\omega_1-\omega_2)/R(\omega_1-\omega_2)$ in low-pressure N_2 studies. However, this referencing technique does not take into account the spectral and intensity distributions of the ω_2 laser modes because the nonlinear response of the rare gas is independent of $(\omega_1-\omega_2^k)$. Furthermore, the saturation effects which take place in the sample channel are totally absent in the reference, which causes an unbalance.

Replacing rare gas referencing by referencing in a cell which contains the gas analysed in the sample channel solves the problem completely. The reference signal is now also given by (1). In order to obtain a ratio $S(\omega_1-\omega_2)/R(\omega_1-\omega_2)$ which is proportional to the ratio $\Delta N_J^S/\Delta N_J^R$, where ΔN_J^R is the population difference in the reference cell, and independent of the laser powers, precise conditions have to be fulfilled.

First, the expression inside the integral equation (1) must be the same for the sample and the reference channels. This is fulfilled when collisional broadenings are the same in both channels and when Doppler broadenings are comparable. Because the collisional broadenings depend strongly on the collisional partners and the temperature, it is difficult to maintain similar broadenings in both channels, especially during combustion experiments for which the local gas mixture and temperature may change rapidly. At low pressures, the above conditions are easily fulfilled because collisional broadenings are negligible. One requires only the translational temperatures to be close in both cells. Second, saturation must have the same effects in both channels, i.e. their respective S_{AT} terms must be equal. This implies that the power densities at the probe volumes have to be as close to each other as possible. We will see later the effect of a temperature difference on experimental results and how close the power densities have to be.

We now deduce the rotational temperature from the signal intensities when the above hypotheses are fulfilled. Also the temperature accuracy is derived.

Temperature Derivation and Temperature Measurement Accuracy

We calculate the ratios Q_1, Q_2, and Q where:

$$Q_1 = S(\omega_1-\omega_2)/R(\omega_1-\omega_2), \tag{6a}$$

$$Q_2 = S(\omega_1-\omega_2')/R(\omega_1-\omega_2'), \tag{6b}$$

$$Q = Q_1/Q_2 . \tag{6c}$$

Replacing the probe and reference signals by their expressions according to (1) we obtain:

$$Q = (K_S K_R'/K_R K_S')(\Delta N_J^S \Delta N_{J'}^R/\Delta N_J^R \Delta N_{J'}^S)^2 . \tag{7}$$

The population differences are written as functions of the vibrational and rotational terms $G(v)$ and $F_v(J)$, respectively. For ΔN_J^s we obtain:

$$\Delta N_J^s = N_0^s\left[\exp\left(-\frac{F_0(J)}{kT^s}\right)\exp\left(-\frac{G(0)}{k\theta^s}\right) - \exp\left(\frac{F_1(J)}{kT^S}\right)\exp\left(-\frac{G(1)}{k\theta^S}\right)\right] \tag{8}$$

where N_0^s is the number density of molecules, T^S and θ^S are the rotational and vibrational temperatures in the signal cell. k is the Boltzmann constant. Expression (8) assumes that the rotational temperature does not depend on the vibrational states. Writing similar equations for ΔN_J^R, $\Delta N_{J'}^S$, and $\Delta N_{J'}^R$ and neglecting the rotational-vibrational coupling, we get:

$$Q = (K_S K_R'/K_R K_S')\exp[-(2\Delta E/k)(1/T^S - 1/T^R)] \tag{9}$$

where $\Delta E = F_0(J) - F_0(J')$.

The rotational temperature in the reference cell being known, we derive T^S:

$$T^S = \frac{\Delta E/k}{\frac{1}{2}\ln Q + \frac{\Delta E}{kT^R} - \frac{1}{2}\ln A} \tag{10}$$

where $K_S K'_R / K_R K'_S$ has been replaced by A which is deduced from an experiment carried out in a gas at known temperature. Expression (9) also yields

$$\frac{\Delta T^S}{(T^S)^2} = -\frac{1}{2}\frac{k}{\Delta E}\frac{\Delta Q}{Q} \tag{11}$$

where $\Delta Q/Q$ is the relative uncertainty of the measurement.

Experimental Setup

The core of the system is a single-mode Q-switched Nd:YAG laser chain which delivers 800 mJ of I.R. in 15 ns pulses. This output is frequency doubled in two KDP crystals, giving a total of 220 mJ at 532 nm. Some 40 mJ are used to pump two narrow-band dye oscillators (ω_2 and ω'_2 frequencies) each followed by one amplifier. About 50 mJ are used to pump each of the dye amplifiers, whereas the remainder (80 mJ) is used as the ω_1 beam.

The resonator of the ω_2 laser comprises a 2400 gr/mm holographic grating at grazing incidence and a flat rotating back mirror. The linewidth is 0.25 cm^{-1} full width at half maximum (FWHM). The ω'_2 resonator comprises a 2400 gr/mm grating at Littrow incidence as back mirror, and two intracavity solid Fabry-Pérot étalons. They are 0.1 mm and 1 mm thick, respectively. The ω'_2 laser linewidth is 0.2 cm^{-1} (FWHM).

The optical arrangement of the dye lasers is designed to ensure a good mechanical stability. Most of the optical components of the laser chains are common, viz the output mirror of the oscillator, the dye cell windows, the telescope. Since the output mirror is common for both lasers, the ω_2 and ω'_2 beams are already parallel. They are made to overlap on a dichroic mirror. Then they are mixed on a second dichroic mirror with the ω_1 beams in a planar BOXCARS geometry. At the output of the CARS bench, the available energies are 30 mJ, 30 mJ, 3 mJ, and 3 mJ for the two ω_1 beams and the ω_2 and ω'_2 beams, respectively. The pulse durations are ~12 ns. The laser frequencies are measured with a Fizeau wavemeter (Laser technics).

First, the beams are focussed by means of a 500 mm focal length achromat in the reference cell filled with 10^3 Pa of N_2. Then they are focused again by means of a 250 mm achromat in the sample cell (Fig. 2), after splitting off the anti-Stokes beams generated in the reference cell using a dichroic mirror.

Reference and sample CARS beams are dispersed in two separate 0.8 m spectrometers each equipped with a concave, 50 mm-diameter, 2100 gr/mm holographic grating. The CARS spectral lines are imaged with a X4 magnification optics onto two photodiode arrays (EGG512HQ) read by a COMPAQ386/25 computer. The spectral dispersion is 0.125 cm^{-1}/diode and the resolution is 0.5 cm^{-1} (FWHM).

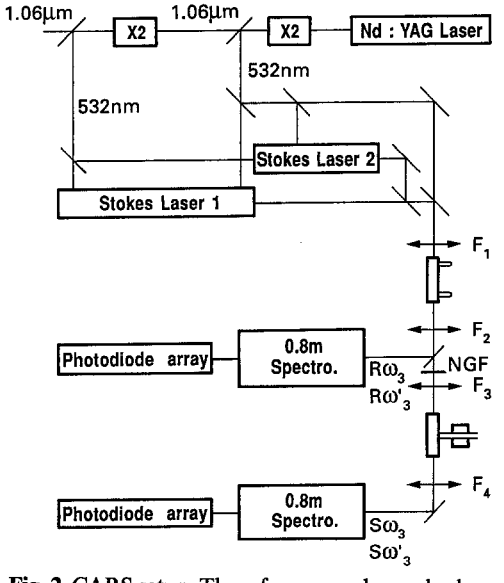

Fig. 2. CARS setup. The reference and sample channels are mounted in "series". (F_1, F_2: 500 mm focal length achromats; F_3, F_4: 250 mm focal length achromats. NGF: neutral glass filter)

Experimental Choices

We here discuss successively several technical points. First we define the saturation effects which can be tolerated. Secondly, we choose the rotational lines which the lasers have to be tuned to.

To obtain measurable anti-Stokes signals from low-concentration molecular gas, high-power lasers always have to be used. As a consequence saturation effects cannot be avoided in dual-line CARS experiments. This is demonstrated in Fig. 3 where $\overline{S_{AT}}$ (S_{AT} is here averaged over 15 laser shots) fails to reach a constant value when the density product $(I_1 I_2)^{1/2}$ is reduced to its minimum practical value before signal disappears. Note however that earlier experiments showed that saturation becomes negligible for $(I_1 I_2)^{1/2} = 10^9$ W/cm^2 [10]. Experimentally S_{AT} has been measured for the N_2 $Q(8)$ line, within a proportionality constant, by dividing the intensities of two signals recorded, respectively, in nitrogen at 2.1 10^2 Pa and in argon. I_1 and I_2 are derived by assuming

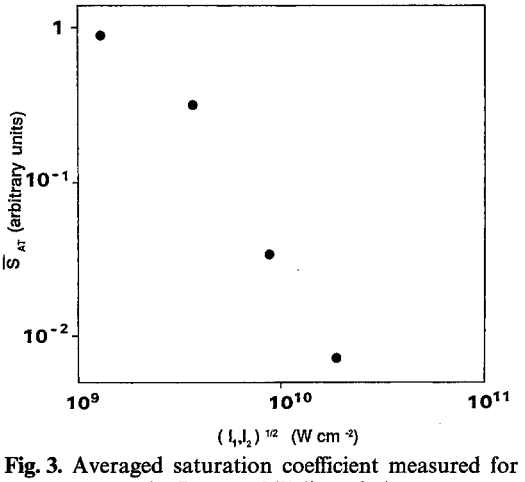

Fig. 3. Averaged saturation coefficient measured for $(\omega_1 - \omega_2)$ on resonance on the Raman $Q(8)$ line of nitrogen

the laser beams to have a divergence of 1.3 times the diffraction limit (this divergence was measured earlier [10]). $I_1 I_2$ is changed from its nominal value of $\sim 2\,10^{10}$ W/cm^2 by inserting neutral glass filters on the beams between the two probe volumes. During the experiment a large value for I_1, viz $I_1 = 400\, I_2$, is kept to take advantage of the dependence of the signal strength on the laser densities. Even then, the signal strength at $2.1\,10^2$ Pa is too weak to be usable for $I_1 I_2 < 10^9$ W/cm^2, when using 250 mm focal lenght achromat.

Obviously, saturation effects would not impair the temperature measurement accuracy of dual-line CARS when the power densities at sample and reference probe volumes are equal. However, it is experimentally difficult to keep these power densities equal to within 10% or better. Therefore it is important to define what level of saturation is tolerable.

Saturation effects are generally discussed [10] using the Stark frequency Ω_S and the Rabi frequency Ω_R; it can be shown that: (i) the Raman line chirps during the laser pulse and its shift at the peak of the laser pulse is Ω_S; (ii) the population difference between the CARS-coupled vibrational states is driven into an oscillation which causes a signal reduction and a broadening of the CARS line. The signal reduction is significant when $\Omega_R\, \tau_p \gtrsim 1$ where τ_p is the pulse duration; the broadening becomes visible when Ω_R exceeds the Doppler linewidth $\Delta\omega_D$.

Because we here maintain $I_1 = 400\, I_2$, the Stark effect is mainly caused by the ω_1 beam and Ω_S is practically proportional to the ω_1 power density. From [10] we calculate that Ω_S increases from $3 \cdot 10^{-3}$ cm^{-1} for

$(I_1 I_2)^{1/2} = 10^9$ W/cm^2

to $3 \cdot 10^{-2}$ cm^{-1} for

$(I_1 I_2)^{1/2} = 10^{10}$ W/cm^2;

also $\Omega_R \simeq 0.1\, \Omega_S$. With $\Delta\omega_D \sim 5 \cdot 10^{-3}$ cm^{-1}, Ω_S exceeds the Doppler linewidth and is comparable to the free spectral range between the ω_2^K modes ($\delta\omega_2^K \simeq 10^{-2}$ cm^{-1}). Also, with $\tau_p \simeq 12$ ns, Raman pumping is significant although Rabi broadening can be neglected. The Ω_R and Ω_S frequencies obtained in the sample and reference channels differ by the same amount as the power densities, i.e. by 10% under our hypothesis. These disparities will remain acceptable as long as (i) the two signals are mainly created by the same ω_2^K mode: $0.1\, \Omega_S \ll \delta\omega_2^K, \Delta\omega_D$ and (ii) the Raman pumpings remain close, viz $0.1\, \Omega_S \tau_p \ll 1$.

A good compromise between signal strength and saturation effects is obtained empirically for

$(I_1 I_2)^{1/2} = 5.6\, 10^9$ W/cm^2.

with $I_1 = 1.2\, 10^{11}$ W/cm^2 and $I_2 = 2.6\, 10^8$ W/cm^2. Our results show also that the relative standard deviation σ_{Q_1} of Q_1 is smaller than 5% with disparities in power densities in sample and reference probe volumes as large as 10%.

The set of two rotational lines must be selected to optimize the temperature accuracy. Equation (11) shows that it is advantageous to increase ΔE. However this may degrade the signal/noise ratio on Q_1 or Q_2 or both and a compromise has to be found. In practice, two factors reduce the signal/noise ratio for high J levels:

1) High J states are little populated; the signal is weak and Poisson statistics affect the measurement accuracy;

2) Even when a $Q(J)$ line is intense, it may appear on a coherent weakly resonant background due to the other J lines and which is not suppressed by non-resonant background suppression technique. Then (1) is not valid to estimate the CARS signal of the $Q(J)$ line. By recording N_2 CARS spectra with the scanning CARS technique, we observe that below $J = 8$ the Q-lines overlap partially when the spectral resolution is of the order of 0.1 cm^{-1}. Also, for $J > 16$, the signal/noise ratio decreases quickly when the rotational temperature is below 300 K. Therefore we select for our study the $Q(8)$ and $Q(16)$ lines.

Experimental Results

First, studies of the pulse to pulse reproducibility of the Q_1 ratio are performed because the temperature accuracy depends on $\Delta Q/Q$ and, consequently, on $\Delta Q_1/Q_1$ and $\Delta Q_2/Q_2$. The reference cell is filled with 10^3 Pa of N_2 at 293 K. The $(\omega_1 - \omega_2)$ frequency is tuned on resonance with the $Q(8)$ line. From 20 single-pulse measurements of Q_1 we deduced the average value $\langle Q_1 \rangle$ and the standard deviation σ_{Q_1}. σ_{Q_1} is found to be close to the shot noise limit, as seen in Fig. 4 where the number of the photocounts in the sample channel is changed by inserting calibrated neutral glass filters on the anti-Stokes beam while the reference signal is maintained close to 5000 photocounts. The slight excess over the shot noise limit may be due to slight differences in the optical conditions at the two probe volumes:

1) the beam overlap is not strictly the same because the effects of the diffraction and direction instability of the beams are not exactly compensated. This is because optical (geometrical and dispersive) aberrations are added by the optics located between the two foci;

2) the population pumping and the Stark effect are different. This latter explanation is confirmed by the fact

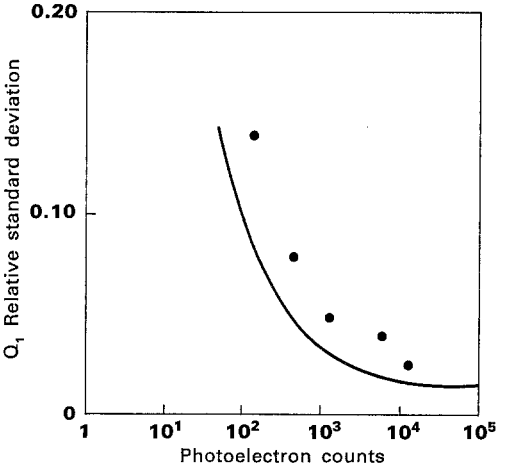

Fig. 4. Standard deviation σ_{Q_1} versus the number of photoelectrons detected in the signal channel (Signal cell: 10^3 Pa of N_2 at 293 K. Solid line: theoretical prediction of σ_{Q_1} when the Q_1 fluctuations are only due to Poisson statistics)

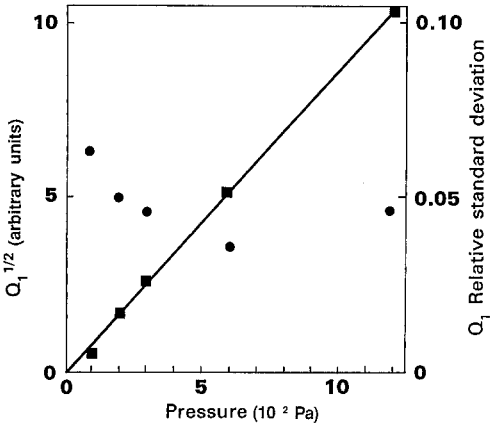

Fig. 5. Average value (■) and standard deviation (●) of Q_1 versus N_2 pressure in the sample cell. Reference cell pressure: 10^3 Pa. Temperature in both channels: 293 K. The frequency difference $(\omega_1-\omega_2)$ is tuned on the $Q(8)$ line

that σ_{Q_1} decreases by 20% when N_2 is replaced by argon simultaneously in both channels, i.e. when the saturation effects disappear.

σ_{Q_1} is also found (Fig. 5) to be independent of the pressure of the signal cell in the range 10^2–$1.2\cdot10^3$ Pa when the pressure of the reference cell is maintained at 10^3 Pa. This result is important since, in practice, the pressures in the reference and sample cells may be different. However, the result was expected because the Raman lineshapes remain essentially Doppler-broadened whatever the pressure in the pressure range which is analyzed. Note also that $\langle Q_1\rangle^{1/2}$ is proportional to the pressure, which demonstrates that number density measurements can be done.

We now have to assess quantitatively the standard deviation σ_Q of Q. Obviously, σ_Q depends on σ_{Q_1} and σ_{Q_2} but partial correlation may exist between Q_1 and Q_2 fluctuations because the ω_1 beam interacts with both ω_2 and ω_2' beams. Two experimental setups were tried to generate the ω_2 and ω_2' frequencies:

- each frequency is created independently by a dye laser (solution #1). Each line is multimode and $\sim0.2\ \mathrm{cm}^{-1}$ broad.
- both frequencies are created by one dye laser which emits simultaneously two multimode bands, each of them being $\sim0.2\ \mathrm{cm}^{-1}$ wide (solution #2).

Solutions #1 and #2 are compared by measuring σ_Q, σ_{Q_1}, and σ_{Q_2} during an experiment in which the sample and reference cells are filled with argon. Therefore the effects of saturation and exact mode position can be ignored. Solutions #1 and #2 yield equivalent standard deviations (Table 1). The dye laser with grazing incidence grating gives slightly higher standard deviations, probably because its beam has a poorer geometrical quality. More important, whatever the solution, σ_Q is comparable to or smaller than σ_{Q_1} and σ_{Q_2}, which demonstrates that the fluctuations of Q_1 and Q_2 are partially correlated. On the other hand, solutions #1 and #2 give rise to different values of σ_Q when the beams are perturbed along their paths to the probe volume. The latter situation is simulated by blowing hot air (700 K) just before the achromat which focuses the beams at the sample probe volume. The perturbation to the beam propagation is adjusted to be so severe that $\langle Q_1\rangle$ and $\langle Q_2\rangle$ are reduced by a factor 3 and that σ_{Q_1} and σ_{Q_2} increase approximately tenfold. The results of the solution #1 are more sensitive to the perturbation than those of the solution #2 because in the latter case the geometries of the ω_2 and ω_2' beams are perfectly matched. It has also been observed that with solution #2, $\langle Q\rangle$ and σ_Q are nearly insensitive to slight misalignments between the (ω_2, ω_2') and ω_1 beams.

Table 1. Relative standard deviations of the Q_1, Q_2, and $Q=Q_1/Q_2$ ratios for different experimental arrangements (see text)

		σ_{Q_1}	σ_{Q_2}	σ_Q
Solution #1	without disturbance	0.03	0.07	0.06
	with disturbance	0.40	0.40	0.35
Solution #2	without disturbance	0.02	0.02	0.025
	with disturbance	0.20	0.25	0.06

As a consequence of the above findings, the solution #2 is used during the following experiments.

As first test of dual-line CARS, single-shot rotational temperature measurements are performed in a low-pressure warm flow in thermal equilibrium. The reference and sample cells contain N_2 gas at a pressure of $1.25\cdot10^3$ Pa. The temperature is maintained at 293 K in the reference cell and can be varied in the sample cell. The latter consists of a 10 mm-internal-diameter glass tube. It is heated by the Joule effect. The internal temperature is controlled by a chromel-Alumel 0.3 mm-diameter thermocouple located 5 mm from the probe volume.

The ω_2 and ω_2' frequencies are emitted by the laser which is spectrally narrowed by the grating in Littrow configuration (Chap. 2). The 0.1 mm-thick Fabry-Pérot étalon is removed from the cavity whereas the 1 mm-thick étalon is conserved. Then the laser emits two narrow lines which are approximately $0.2\ \mathrm{cm}^{-1}$ broad. The first one (ω_2') is tuned so that $(\omega_1-\omega_2')=2325.20\ \mathrm{cm}^{-1}$, i.e. to the $Q(16)$ Raman frequency $(\omega_1=18789.40\ \mathrm{cm}^{-1}$; $\omega_2'=16464.20\ \mathrm{cm}^{-1})$. The second one (ω_2), is centered at $16460.82\ \mathrm{cm}^{-1}$, one free spectral range of the 1 mm-thick Fabry-Pérot étalon away from ω_2'. So $(\omega_1-\omega_2)$ $=2328.58\ \mathrm{cm}^{-1}$, close to $Q(8)$ Raman shift of $2328.67\ \mathrm{cm}^{-1}$. Because of this slight detuning, the $Q(8)$ CARS signal is reduced and becomes nearly equal to the $Q(16)$ signal strength; this facilitates their detection using a photodiode array, because the latter has limited dynamic range.

Figure 6 shows a good agreement between the dual-line CARS temperature and that given by a thermocouple. Each CARS temperature is the average of 15 single-shot temperature measurements. The ability of the dual-line technique for single-shot measurements is demonstrated by the small standard deviation of the instantaneous temperatures. Standard deviations are close to 3–4%. They increase to 6% when $T_{ROT}>600$ K. This is because the signal strengths then become lower than 1000 photoelectrons and also because Doppler effects in the two channels become slightly different.

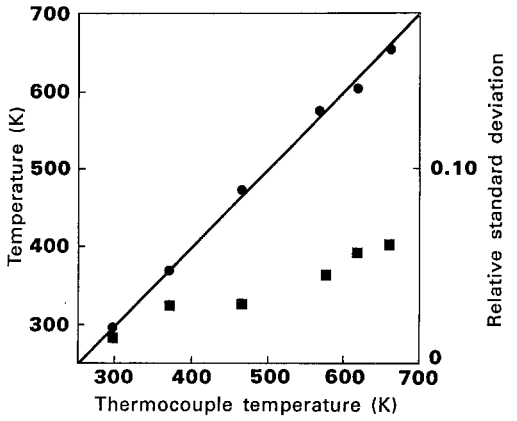

Fig. 6. Average (●) and standard deviation (■) of single-shot dual-line CARS temperature versus temperature measured by a thermocouple (Cell pressures: $1.25\,10^3$ Pa. Reference cell temperature: 293 K)

Conclusion

We have demonstrated that dual-line CARS allows accurate single-shot rotational temperature measurement in a low-pressure flow. The tests were carried out for N_2 at pressures of the order of 10^3 Pa. At the present time, the detectivity is approximately limited to the range 10^2–10^4 Pa. For the present work, short focal length achromats have been used which make it necessary to use limited laser powers to maintain acceptable saturation. By introducing longer focal lengths, experiments could easily be performed with the same accuracy at pressures below 10^2 Pa, but at a cost in spatial resolution.

Further, the demonstration has been given for rotational temperature measurements in the range 300–700 K. Dual-line CARS could be used at higher temperatures as long as enough photoelectrons are collected and provided a hot reference cell is used in order to maintain similar Doppler broadening in signal and reference channels. It would readily be adapted for vibrational temperature measurement provided we replaced the static reference cell by an N_2 glow discharge in order to have an appreciable population in the $v=1$ state.

Further work is also needed to optimize the measurement accuracy in the low rotational temperature flows which are produced by low enthalpy hypersonic tunnels. Then the choice of the rotational lines will become more difficult if only the first rotational lines are populated. The use of pure rotational transitions may then prove superior.

Acknowledgements. The authors are very grateful to J. P. Taran for helpful discussions, to P. Bouchardy for expert computational assistance and to G. Collin and P. Magre for their hospitality.

The work has been carried out under a DRET contract, French Ministry of Defense.

References

1. R.K. Hanson: 21st Symposium (international) on Combustion, The Combustion Inst. (1986) p. 1677
2. G. Laufer, R.L. McKenzie: AIAA Paper -88-4679-CP (September 1988)
3. R.J. Exton, M.E. Hillard: Appl. Opt. **25**, 14 (1985)
4. P.R. Régnier, J.P. Taran: Appl. Phys. Lett. **23**, 240 (1973)
5. R.J.H. Clark, R.E. Hester (eds.): Advances in Nonlinear Spectroscopy, Vol. 15 (Wiley, Chochester 1988)
6. M. Aldén, K. Fredriksson, S. Wallin: Appl. Opt. **23**, 2053 (1984)
7. M. Aldén: Sov. J. Quantum Electron. **18**, 746 (1988)
8. R.K. Hanson, J.M. Seitzman, P.H. Paul: Appl. Phys. B **50**, 441 (1990)
9. S. Druet, J.P. Taran, C. Bordé: J. Physique **40**, 819 (1979)
10. M. Péalat, M. Lefebvre, J.P. Taran, P.L. Kelley: Phys. Rev. A **38**, 1948 (1988)
11. R.P. Lucht, R.L. Farrow: J. Opt. Soc. Am. B **6**, 2313 (1989)
12. V.M. Baev, G. Gaida, H. Schröder, P.E. Toschek: Opt. Commun. **38**, 309 (1981)